Dissimilatory nitrate reduction to ammonium coupled to Fe(II) oxidation in sediments of a periodically hypoxic estuary

Elizabeth K. Robertson,*[1] Keryn L. Roberts,[2] Laurine D. W. Burdorf,[3] Perran Cook,[2] Bo Thamdrup[1]
[1]Nordic Centre for Earth Evolution (NordCEE), Department of Biology, University of Southern Denmark, Odense M, Denmark
[2]Water Studies Centre, School of Chemistry, Monash University, Clayton, Victoria, Australia
[3]Royal Netherlands Institute for Sea Research (NIOZ), Yerseke, Netherlands

Abstract

Estuarine sediments are critical for the remediation of large amounts of anthropogenic nitrogen (N) loading via production of N_2 from nitrate by denitrification. However, nitrate is also recycled within sediments by dissimilatory nitrate reduction to ammonium (DNRA). Understanding the factors that influence the balance between denitrification and DNRA is thus crucial to constraining coastal N budgets. A potentially important factor is the availability of different electron donors (organic carbon, reduced iron and sulfur). Both denitrification and DNRA may be linked to ferrous iron oxidation, however the contribution of Fe(II)-fueled nitrate reduction in natural environments is practically unknown. This study investigated how nitrate-dependent Fe^{2+} oxidation affects the partitioning between nitrate reduction pathways using ^{15}N-tracing methods in sediments along the salinity gradient of the periodically hypoxic Yarra River estuary, Australia. Increased dissolved Fe^{2+} availability resulted in significant enhancement of DNRA rates from around 10–20% total nitrate reduction in control incubations to over 40% in those with additional Fe^{2+}, at several sites. Increases in DNRA at some locations were accompanied by reductions in denitrification. Significant correlations were observed between Fe^{2+} oxidation and DNRA rates, with reaction ratios corresponding to the stoichiometry of Fe^{2+}-dependent DNRA. Our results provide experimental evidence for a direct coupling of DNRA to Fe^{2+} oxidation across an estuarine gradient, suggesting that Fe^{2+} availability may exert substantial control on the balance between retention and removal of bioavailable N. Thus, DNRA linked to Fe^{2+} oxidation may be of general importance to environments with Fe-rich sediments.

Estuaries are key regions for the recycling of fixed nitrogen (N) compounds—effectively remediating large proportions of excessive nutrient loading before it reaches the open oceans (Boynton and Kemp 2008; Howarth et al. 2011). In these environments, the anaerobic pathways denitrification, anaerobic ammonium oxidation (anammox), and dissimilatory nitrate reduction to ammonium (DNRA) regulate the fate of introduced N in sediments. These pathways compete for nitrate and nitrite (NO_x); their relative contribution to NO_x reduction ultimately determining whether nitrogen inputs are recycled to the atmosphere as N_2 by denitrification and/or anammox or remains bio-available as ammonium through DNRA. Denitrification has been long recognized as a major sink for nitrate in estuaries, providing a key ecosystem service by removing large amounts of anthropogenic nitrate. Denitrification here, and in adjacent coastal sediments thus removes a large proportion of introduced N before it reaches the open oceans (Seitzinger et al. 2006; Howarth et al. 2011). In contrast, a dominance of DNRA, as observed in some studies on coastal sediments (e.g., An and Gardner 2002; Dong et al. 2011; Dunn et al. 2013), results in the net retention of N in sediments where it can be potentially be released and turned over, leading to increased N loading, eutrophication and associated deleterious effects. The relative contribution of denitrification and DNRA is highly variable between different locations, however we have no firm understanding of what regulates this ratio (Giblin et al. 2013).

With increasing anthropogenic perturbations imposed on global N cycling, there is a clear need to investigate the controls on the partitioning between denitrification and DNRA. To date most work has focused on the role of organic matter (e.g., Brettar and Rheinheimer 1992; Yin et al. 2002; Nizzoli et al. 2010) and NO_x availability (Koop-Jakobsen and Giblin 2010; Dong et al. 2011; Kraft et al. 2014) in controlling the relative importance of these processes. DNRA has been

*Correspondence: elizabeth.k.robertson@gmail.com

suggested to be favored over denitrification under more reduced conditions such as those caused by high carbon loading (Burgin and Hamilton 2007; Giblin et al. 2013). The process might be coupled directly to organic carbon oxidation under such conditions, but could also result from increased availability of inorganic electron donors such as sulfide which may act as a reductant for DNRA (e.g., Brunet and Garcia-Gil 1996; An and Gardner 2002) while inhibiting denitrification (e.g., Sørensen et al. 1980; Jensen and Cox 1992).

Fe^{2+} may also serve as an electron donor in several steps in anaerobic nitrogen cycling and may influence the fate of N in sediments. The coupling of NO_x reduction to Fe^{2+} oxidation has been shown in numerous microbial strains (Straub et al. 1996; Kappler et al. 2005; Chakraborty et al. 2011) and sediment enrichments (Weber et al. 2006b; Coby et al. 2011) and may provide comparable energetic gains as oxidation of organic substrates such as acetate (Table 1). The majority of microbial isolates studied to date appear to reduce NO_x to N_2 while oxidizing Fe^{2+} (e.g., Straub et al. 1996; Kappler et al. 2005; Chakraborty and Picardal 2013b). However, some studies investigating the capacity for iron driven nitrate reduction in mixed microbial communities of enriched sediment have shown that NH_4^+ may also be produced during Fe^{2+} oxidation (Weber et al. 2006b; Coby et al. 2011).

In addition the microbial coupling of NO_x reduction and Fe^{2+} oxidation, several mechanisms of Fe^{2+}-fueled NO_x reduction have been identified that involve abiotic processes (e.g., Carlson et al. 2012; Picardal 2012). Abiotic reactions involving surface catalysis have been shown to produce N_2, N_2O and NO (Moraghan and Buresh 1977; Sørensen and Thorling 1991; Coby and Picardal 2005) or NH_4^+ (Hansen et al. 1996; Ottley et al. 1997; Rakshit et al. 2005) as end products from the oxidation of a range of Fe^{2+} substrates. Green rusts, in particular, can reduce nitrate abiotically at rates comparable to that of microorganisms (Dhakal et al. 2013). Green rusts may also form during microbially mediated Fe^{2+} oxidation and result in oxidation taking place partly enzymatically and partly indirectly by abiotic interactions (Pantke et al. 2012; Etique et al. 2014).

Despite there being significant attention in the past 15 yr on microorganisms carrying out iron-driven nitrogen cycling (Carlson et al. 2012, 2013; Picardal 2012; refs. above), their contribution to biogeochemical cycling in natural environments remains unknown. Significant correlations have been observed between sediment Fe oxide content and nitrate reducing processes in two coastal bays, with oxidation of Fe^{2+} being suggested in both studies to drive denitrification (Hou et al. 2012; Yin et al. 2014). Recently, Roberts et al. (2014) measured shifts in dominant nitrate reducing process depending on whether sediment cores were maintained under oxic or anoxic conditions. In that study, Fe^{2+} at 1 cm depth in the porewater increased from < 5 μmol L^{-1} under

an anoxic water column to >400 μmol L^{-1} under oxic conditions. These observations lead to the suggestion that relatively higher DNRA rates observed during oxic conditions may to be linked to higher availability of Fe^{2+}.

Here, we investigated the pathways and dynamics of iron-driven nitrate reduction in the iron-rich sediments of the Yarra River estuary, Australia. Anoxic slurries of surface sediments were amended with ^{15}N-labeled substrates to accurately quantify process rates of denitrification and DNRA and their possible coupling to the oxidation of Fe^{2+}. From experimental observations we provide evidence of Fe^{2+}-driven nitrate reduction to ammonium based on process rates and reaction stoichiometries, which may have important implications for nitrogen cycling in natural environments.

Methods

Sampling

Cores and bottom water samples were taken from five locations along the Yarra River estuary during summer (January–March) 2014 (Fig. 1). The salt wedge structure can extend up the river for up to 22 km, causing periodic hypoxia and anoxia in saline bottom waters, especially during periods of low river discharge (Roberts et al. 2012). Sites were selected along the river's salinity gradient, from the fully marine site E ("Bay"; 37°51′ 12.3″S 144°54′ 28.6″E) and covering the extent of the salt wedge (site D, "Morell Bridge"; 37°49′39.5″S, 144°59′05.0″E; site C, "Scotch College"; 37°50′00.1″S, 145°01′35.5″ E; site B, "Bridge Road"; 37°49′09.8″S, 145°00′53.7″E) to a freshwater site (site A, "Yarra Bend"; 37°47′57.60″S, 145° 0′23.73″E) separated from any marine influence by an artificial barrier (Dight's Falls, Fig. 1). Sediment cores were collected in 27.5 × 6.6 cm i.d. polyethylene core liners using a manual corer, and sealed with rubber stoppers. Bottom water was collected using a 5 L Niskin bottle for use in sediment incubations. Samples of bottom water (~10 mL) to determine in situ nutrient concentrations were filtered (0.2 μm) and frozen until later analysis. Cores and water samples were returned to Monash University where they were stored within 4°C of in situ water temperature (Table 2). Water column profiles of chemical parameters (dissolved oxygen, salinity, pH) were measured using a multimeter (U-10 Horiba) during sampling at each site.

Sediment profiles

Triplicate cores were sectioned (0.5 cm intervals in the upper 3 cm, 1 cm intervals at 3–6 cm) immediately after returning from the field at four of the five sites. Cores from site E were aerated overnight to maintain them at in situ oxygen concentration before being sectioned due to time constraints. Sediment was centrifuged (2000 rpm for 5 min) and the pore water was filtered (0.2 μm) and preserved for later nutrient, sulfide and iron analyses, all with rapid processing to minimize oxidation. Samples for free sulfide were

Table 1. Reaction stoichiometries normalized to nitrogen compounds and standard free energy yields of NO_x reduction processes linked to Fe^{2+} oxidation compared with oxidation of an organic substrate (acetate). Calculated from Stumm and Morgan (1981).

Equation	Reaction	$\Delta G^{o'}$ (kJ mol^{-1} NO_x)
1	$NO_3^- + 5\ Fe^{2+} + 12\ H_2O \rightarrow 1/2\ N_{2\ (g)} + 5\ Fe(OH)_3 + 9\ H^+$	-503
2	$NO_3^- + 8\ Fe^{2+} + 21\ H_2O \rightarrow NH_4^+ + 8\ Fe(OH)_3 + 14\ H^+$	-508
3	$NO_2^- + 3\ Fe^{2+} + 7\ H_2O \rightarrow 1/2\ N_{2\ (g)} + 3\ Fe(OH)_3 + 5\ H^+$	-363
4	$NO_2^- + 6\ Fe^{2+} + 16\ H_2O \rightarrow NH_4^+ + 6\ Fe(OH)_3 + 10\ H^+$	-368
5	$NO_2^- + 1/2\ CH_3COO^- \rightarrow 1/2\ N_{2\ (g)} + HCO_3^- + 1/2\ H^+$	-385
6	$NO_2^- + 3/4\ CH_3COO^- + 5/4\ H^+ + H_2O \rightarrow NH_4^+ + 3/2\ HCO_3^-$	-358

fixed with zinc acetate (50 μL 500 μmol L^{-1} in 1 mL sample). Samples for nutrients were frozen. Fe^{2+} samples were preserved with sulfamic acid as in slurry experiments (see below).

Sediment slurry incubations

Sediment slurry experiments were carried out at each station with triplicate incubations of each treatment. One gram of homogenized surface (upper 1 cm) sediment and 99 mL of filtered (GF/F; 0.7 μm, Whatman) site water were added to 120 mL serum vials. Vials were sealed with blue butyl stoppers and aluminum caps, the liquid and gas phases purged with helium (high purity helium, Air Liquide) for 15 min, and placed on a shaker table (~120 rpm) overnight to remove residual oxygen and nitrate. Anoxically prepared $Fe^{II}Cl_2$ solution (1 mL 50 mmol L^{-1}) was added to half of the vials, the pH adjusted to within 0.2 pH units of that of control vials (pH 6.9, 7.3, 7.6, 7.7 and 8.1 for sites A, B, C, D, and E, respectively) by addition of sterile filtered (0.2 μm) 0.5 mol L^{-1} HCl or NaOH. Vials were then returned to the
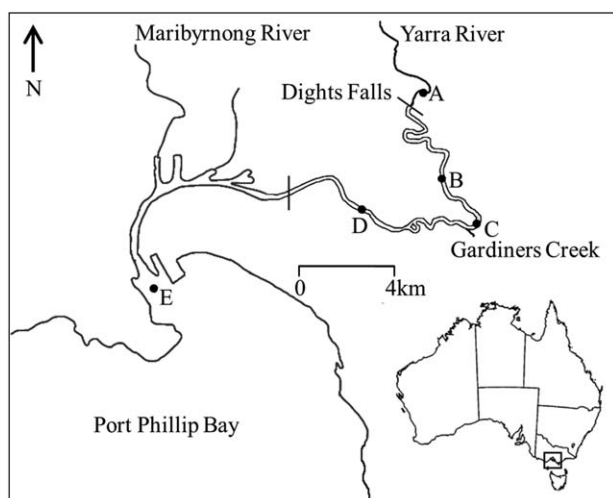

Fig. 1. Location of sampling sites located along the Yarra River estuary, Melbourne, Australia. A: Yarra Bend, B: Bridge Road, C: Scotch College, D: Morell Bridge, E: Bay.

shaker table for 24–48 h. During this time vials were sampled for for both Fe^{2+} and pH to ensure both were stable, before labeled substrates (1 mL 10 mmol L^{-1} Na$^{15}NO_3$ or Na$^{15}NO_2$;->98% ^{15}N; 100 μmol L^{-1} final conc.) were added. Many studies report the use of an organic co-substrate for bacterial growth using iron-fueled nitrate reduction (Straub and Buchholz-Cleven 1998; Kappler et al. 2005; Chakraborty and Picardal 2013a). To assess the use of acetate as a co-substrate in iron-fueled nitrate reduction, and possible contributions of heterotrophic organisms to nitrate reduction, a parallel set of $^{15}NO_3^-$ (+/− $Fe^{II}Cl_2$) incubations were run with the addition of acetate (1 mL of 10 mmol L^{-1} sodium acetate; 100 μmol L^{-1} final conc.).

All sampling and substrate addition took place inside an anaerobic chamber (N_2 atmosphere) to prevent chemical oxidation of iron while transferring from the sealed vials to acid. At each time point, samples for N_2 isotope analysis were taken by sampling 2 mL gas headspace from the vials using a 2.5 mL glass syringe (Hamilton) and hypodermic needle, replacing this volume with helium to avoid overpressure in slurry vials. The gas sample was transferred to 3 mL Exetainers (Labco, UK) that had been filled, before sampling, with He-purged ultrapure water amended with $ZnCl_2$ (final 0.5% w/v L^{-1}) to inhibit any microbial activity. An exhaust needle was pierced through the septum of the filled exetainer and the gas sample was introduced from the syringe, displacing an equal volume of water. Gas samples were stored upside down until later analysis. Additionally, a 5 mL aliquot of liquid phase was sampled for analysis of nutrients (NO_3^-, NO_2^-, total NH_4^+, $^{15}NH_4^+$; 3 mL filtered (0.2 μm), stored frozen) and Fe^{2+} associated with dissolved (filtered sample, 0.2 μm) and particle-associated (unfiltered) phases. Both filterable and solid-phase iron samples were acidified with sulfamic acid to a final concentration of 40 mmol L^{-1} to avoid abiotic oxidation of Fe(II) at low pH in the presence of nitrite, which would enhance apparent rates of iron oxidation and nitrite reduction as an experimental artefact (Coby and Picardal 2005; Klueglein and Kappler 2013). Slurry pH was monitored and maintained by addition of sterile filtered (0.2 μm) 0.5 mol L^{-1} HCl or NaOH throughout the

Table 2. In situ parameters taken at time of sampling and benthic fluxes and denitrification measured in the laboratory. Oxygen, nitrate, and ammonium concentrations represent those determined from bottom water samples. Fluxes and whole core denitrification rates were determined in the laboratory, negative values denote solute uptake. Fluxes: (SD), $n = 4$. Denitrification: (SE linear regression).

	A	B	C	D	E
	(Yarra Bend)	(Bridge Road)	(Scotch College)	(Morell Bridge)	(Bay)
Depth (m)	3.2	2.0	3.5	n/d	3.7
Salinity (surface)	0.01	2.1	n/d	7.0	35.0
Salinity (bottom)	0.01	3.7	26.8	30.9	35.0
Surface water temperature (°C)	20.04	24.1	23.6	23.2	18.0
pH	6.9	7.3	7.6	7.7	8.1
Oxygen (μmol L^{-1})	283.9	168.7	85.6	30.0	295.6
Nitrate (μmol L^{-1})	15.2	5.5	5.6	10.5	0.7
Ammonium (μmol L^{-1})	7.01	0.7	21.3	24.4	1.2
Oxygen flux (mmol m^2 d^{-1})	−13.8 (1.6)	−36.3 (3.1)	−34.1 (3.6)	−46.8 (3.7)	−27.8 (3.3)
Nitrate flux (mmol m^2 d^{-1})	−1.0 (0.5)	−2.6 (0.7)	−2.2 (0.4)	−2.3 (1.2)	0.1 (0.3)
Ammonium flux (mmol m^2 d^{-1})	1.5 (0.4)	6.2 (1.6)	−2.1 (1.6)	6.2 (2.4)	−0.5 (0.2)
Denitrification (μmol N m^2 h^{-1})	93.5 (20.9)	197.8 (92.8)	142.2 (11.2)	24.6 (9.6)	41.6 (60.6)

incubation to maintain pH in the desired range (see above). Following each time point, vials were removed from the glove box and the headspaces flushed with helium to remove N_2 before being returned to the shaker table. A cumulative total of N_2 accumulation was calculated over time.

Rates of denitrification and nitrate and nitrite reduction to ammonium from the slurry experiments were calculated from the initial accumulation of ^{15}N-N_2 and $^{15}NH_4^+$, respectively, over time using linear regression, typically covering the first 48 h after ^{15}N-substrate addition and before substrates were depleted (e.g., Fig. 3). Likewise, rates of nitrate consumption, and the production or consumption of nitrite and Fe^{2+} were calculated by linear regression of the concentrations vs. time for the same time interval.

Fluxes

Nutrient and oxygen fluxes were determined as in Roberts et al. (2012). Briefly, following sampling and returning to the laboratory, cores were aerated overnight at 18°C (within 4°C of in situ temperature; Table 2) to achieve a comparable oxygen concentrations in overlying water at all sites. Following overnight aeration, the majority of the overlying water was removed and replaced with fresh aerated site water. Cores were fitted with free-spinning magnets and the water column stirred via an external rotating magnet. Cores were sealed without air bubbles and oxygen concentrations were monitored over at approximately 0, 1 h, 2 h, and 3 h using a HQ-40d Hach multimeter (Germany). Oxygen concentrations were never allowed to drop below 20% of initial oxygen level. Water nutrient samples were taken at each time point, filtered (0.45 μm) and frozen for later analysis. The

volume removed for nutrient samples was replaced by and equal volume of aerated site water and concentrations corrected for replacement of new water (approximately 1–2% of overlying water volume removed and replaced at each time point).

Intact core ^{15}N incubations

In addition to the slurry incubations, we used the isotope pairing technique (IPT; Nielsen 1992) in whole core experiments to determine denitrification rates at the five sites. It has previously been shown that anammox contributed < 1% to sediment N_2 production in Yarra River sediments (Roberts et al. 2012), thus the contribution of anammox to anaerobic nitrogen cycling was not considered as a significant nitrate removal source in slurry and whole core incubations.

Four cores from each site were used to determine denitrification rates after preincubation with aerated bottom water for at least 6 d in the laboratory to ensure steady state between water column and sediment. Magnetic stirrers were fitted to cores and stirred by an external magnet as before (see Fluxes section), and 250 μL 100 mmol L^{-1} ^{15}N-nitrate added to the overlying water. Nitrate was allowed to equilibrate for approximately 1 h before cores were sacrificed at approximately 0 h, 1 h, and 3 h after the pre-incubation period. Samples were taken for N_2 and NO_3^- analysis as described in Roberts et al. (2012). Briefly, at each time point, cores were opened and a sample for NO_3^- removed from the overlying water, filtered (0.2 μm) and frozen until analysis. Cores were then carefully homogenized so that all the sediment was mixed with the water column to form a slurry. Samples were taken for N_2 analysis by removing ~50 mL of the slurry and overflowing the water sample into a 12 mL Exetainer (Labco, UK). Gas

samples were fixed with $ZnCl_2$ (250 μL 50% w/v to 12 mL sample) to inhibit microbial activity and sealed without air space. A helium headspace was introduced before measurement (approximately 1 week after sampling). N_2 data was corrected for the volume of water in each core using sediment porosity (all sites $\sim$0.8). Denitrification rates were calculated as described in Dalsgaard et al. (2000).

Chemical analyses

Nutrients (NO_x, NO_2^-, NH_4^+) from slurry incubations, fluxes, and pore water profiles were determined by flow injection analysis (FIA; Lachat Quickchem 8000 Flow Injection Analyser, spectrophotometric detector). Concentrations of dissolved and particle-associated Fe^{2+} in slurry experiments and depth profiles were determined photometrically using Ferrozine assay (Stookey 1970; Viollier et al. 2000). Sulfate in pore water was measured on an ion chromatograph (Dionex ICS-2100 with IonPac AS19 column). Sulfide was determined using the methylene blue method (Cline 1969).

N_2 gas samples from experiments with ^{15}N substrate additions were measured on a Sercon 20-22 isotope ratio mass spectrometer connected to a gas chromatograph. The amount of $^{15}N\text{-}NH_4^+$ was determined by conversion of NH_4^+ to N_2 using alkaline hypobromite iodine solution (Risgaard-Petersen et al. 1995). Briefly, samples were diluted in exetainers and the headspaces flushed with helium. Alkaline hypobromite iodine solution was added (25 μL mL^{-1} sample) and the exetainers shaken at room temperature overnight before measuring the gas phase on GC-IRMS as described previously. Standards of $^{15}NH_4^+$ were prepared in parallel with samples to check conversion efficiency and ^{15}N recovery, which was >90%.

Statistical analyses

Data from triplicate slurry incubations were analyzed for significant differences in production or consumption rates of dissolved constituents by comparison using Student's *t*-test in Microsoft Excel. *F* statistics were generated in Microsoft Excel to evaluate linear relationships of Fe^{2+} oxidation with nitrate/nitrite reduction to ammonium and denitrification, respectively. All statistical tests were applied at a 5% confidence level. Hereafter, "significant" is deemed to designate statistical significance at the 5% confidence level unless otherwise noted. Michaelis Menten kinetics of reactions were calculated using GraphPad Prism 6 software.

Results

Site observations

All sites investigated had fine muddy sediments with porosities of $\sim$0.8 (data not shown). Infauna was only observed at the marine site E where burrow-forming polychaete worms (*Nereis* sp.) occurred at high densities. The extent of the salt wedge is clear from surface and bottom water salinity measurements, with the stratification causing depletion in bottom water oxygen concentrations (Table 2). A

typical increase in pH was observed toward the mouth of the estuary due to saltwater intrusion. Nitrate and ammonium were variable between sites, reflecting both the extent of the salt wedge and variations in water inputs between sampling dates. Both nitrate and ammonium were lowest at site E.

Depth profiles of dissolved pore water constituents varied between sites (Fig. 2). Oxygen was consumed within the first millimeters of sediment at sites B, C, and D (L. Burdorf, unpubl. res.). Oxygen profiles were not measured at sites A or E due to high numbers of bioturbating organisms, at site E, and stones. Nitrate and nitrite were consumed within the first few millimeters of sediment (data not shown). Surface (0–1 cm) ammonium concentrations were all below $\sim$250 μmol L^{-1} and ammonium accumulated with depth at sites A, B, and C, indicating the active mineralization of organic matter in deeper layers (Fig. 2; A). Ammonium remained at approximately 200 μmol L^{-1} at site D and 50 μmol L^{-1} at site E throughout the sediment profile.

Surface dissolved Fe^{2+} concentrations were highest at C where Fe^{2+} increased with depth to approximately 800 μmol L^{-1} (Fig. 2; B). Fe^{2+} was also high in surface sediments of site B, accumulating to a lesser degree (generally < 400 μmol L^{-1}) at site A. Lower concentrations (< 100 μmol L^{-1}) of Fe^{2+} were observed throughout the depth profiles at sites D and E with little observable accumulation.

Sulfate profiles generally reflected the extent of saltwater intrusion along the sites investigated, with concentrations increasing toward the mouth of the estuary (Fig. 2; C). Highest sulfate concentrations were generally observed in surface sediments and decreased with depth at sites B and C. The steep gradient in sulfate concentration from $\sim$20 mmol L^{-1} to $\sim$2 mmol L^{-1} at station C may be due to residual lower salinity water in deeper sediment layers rather than sulfate removal by sulfate reducing microorganisms. In sediment cores from sites D and E, no depletion was observed; the sulfate concentration remaining at around 20 mmol L^{-1} throughout cores at both sites. Pore water sulfide was undetectable at all sites and depths except for a small sulfide peak (< 5 μmol L^{-1}) at site E (Fig. 2; D), and at D where it was undetectable at the surface but accumulated to >20 μmol L^{-1} at $\sim$1.5 cm. Given the high Fe content of Yarra River sediment (Fig. 2; B), sulfide produced from sulfate reduction would typically be bound as FeS in sediments and not free in the pore water. The general absence of gradients in pore water constituents at the site E can be attributed to the presence of burrowing organisms irrigating and mixing the sediment.

Benthic fluxes and whole core denitrification rates

Sediment oxygen uptake measured in the laboratory on sediment cores, which had been aerated overnight, varied from 13.8 mmol m^2 d^{-1} at site A to a maximum of 46.8 mmol m^2 d^{-1} at site D (Table 2). Oxygen uptake was highest at the three sites B, C, and D exposed to variations in salinity by the saltwater intrusion, where oxygen was well below
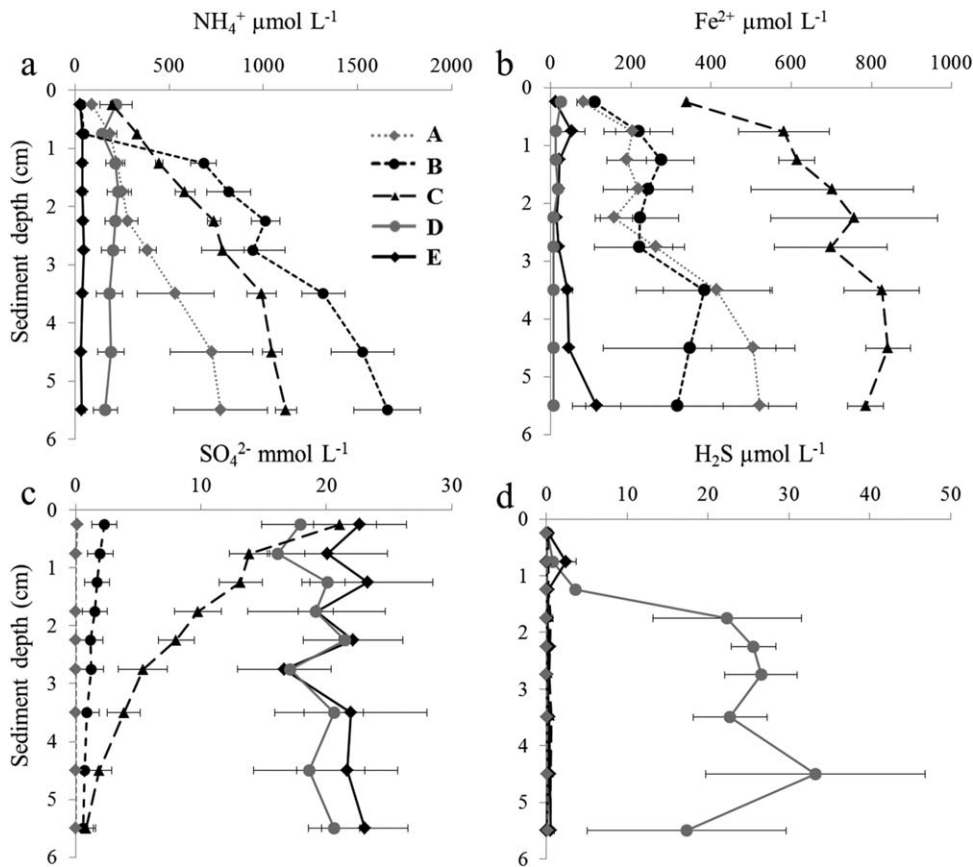
Fig. 2. Depth profiles of sediment pore water constituents from sampling sites. ammonium (**a**); Fe^{2+} in pore water (**b**); sulfate (**c**); H_2S in pore water (**d**). Bars show SD ($n = 3$).

air saturation in situ, such that measured fluxes likely overestimated in situ oxygen uptake. Molecular diffusion was expected to be the main mode of transport due to the absence of irrigating fauna at these sites.

All sites along the estuarine gradient acted as a sink for nitrate (ranging from -1.0 mmol m^2 d^{-1} to -2.6 mmol m^2 d^{-1}) apart from site E where nitrate was depleted in the bottom water and no significant exchange was observed (Table 2). Ammonium fluxes varied greatly along the river with similarly high production observed at sites B and D (both 6.2 mmol m^2 d^{-1}). Net ammonium consumption observed at site C may be due to aeration of cores stimulating nitrification in the surface sediment. Denitrification rates determined after 6 d of aeration (D_{14}, Dalsgaard et al. 2000) ranged from 24.6 μmol m^2 d^{-1} to 197.8 μmol m^2 d^{-1} with the lowest rates at sites D and E with greatest marine influence (Table 2).

Slurry incubations

A consistent pattern of progression of dissolved and gaseous constituents was observed in all slurry incubations with $^{15}NO_x$ substrate additions (Fig. 3). Consumption of added ^{15}N-nitrate or nitrite and accumulation of ^{15}N-labeled reduced products (nitrite, N_2, and ammonium) commenced

immediately after addition. Rates (Table 3) were calculated from the initial, approximately linear production or consumption of dissolved constituents over time, typically the first four time points (within initial 48 h) after ^{15}N-substrate addition (Fig. 3). Rates are presented in μmol L^{-1}, with rates of μmol g sediment^{-1} being approximately 10 times lower due to sediment dilution and slurry volumes.

The concentration of dissolved Fe^{2+} in the slurries without Fe^{2+} amendment varied from 0.2 μmol L^{-1} in slurries from site E to 57 μmol L^{-1} at site C (Table 4). This reflected the relative variation in pore water concentration (Fig. 2), but slurry concentrations were much higher than predicted from dilution of pore water, which is attributed to dissolution from the particle-associated phase. Thus, readily extractable Fe(II) in the particle-associated phase exceeded the dissolved concentration by 1–2 orders of magnitude (Table 4). At all stations, and for all treatments, no changes were observed in this large particulate Fe(II) pool during the slurry incubations (data not shown).

^{15}N substrate and acetate addition

In slurry incubations with ^{15}N-nitrate added, nitrate was consumed immediately on addition at all sites, and it was
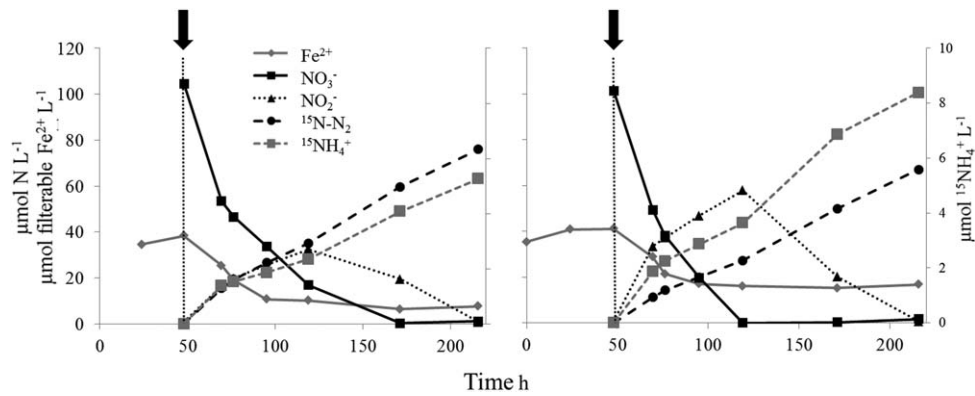
Fig. 3. Example of a typical time series of dissolved constituents in two slurry incubations. Time points from representative slurry incubations with sediment from Bridge Road with 100 μmol L^{-1} ^{15}N-nitrate (left panel) and 100 μmol L^{-1} ^{15}N-nitrate and 500 μmol L^{-1} Fe^{2+}Cl$_2$ (right panel). Black arrow and dotted line represent the time at which ^{15}N-nitrate was added to incubations.

Table 3. Summary of average rates of production (positive values) and consumption (negative values) of dissolved constituents from slurry experiments with standard deviations (SD) $n = 3$.*: $n = 2$†: incubations with acetate (Ac) with low initial nitrite build up followed by rapid depletion giving negative values in rate calculations.

Site	^{15}NO$_3^-$	^{15}NO$_3^-$+Fe^{2+}	^{15}NO$_3^-$+Ac	^{15}NO$_3^-$ + Ac + Fe^{2+}	^{15}NO$_2^-$	^{15}NO$_2^-$ + Fe^{2+}	Fe^{2+} control
Rate (μmol L slurry^{-1} d^{-1})							
A (Yarra Bend)							
Nitrate	−15.4 (2.3)	−21.4 (0.9)	−34.6 (0.7)	−33.6 (2.0)	n/d	n/d	n/d
Nitrite	8.4 (1.7)	13.6 (0.4)	−3.5 (0.1)†	−2.9 (0.2)†	−7.5 (0.7)	−12.9 (0.3)	n/d
Fe^{2+}	−1.0 (0.6)	−1.2 (0.2)	−1.0 (0.8)	−0.7 (0.6)	−1.3 (1.0)	−1.0 (0.2)	−0.2 (1.5)
B (Bridge Road)							
Nitrate	−35.4 (1.7)	−41.8 (2.3)	−52.1 (3.9)	−55.9 (1.5)	n/d	n/d	n/d
Nitrite	12.6 (1.3)	22.1 (1.3)	−0.4 (0.3)†	−2.7 (1.0)†	−28.9 (2.9)	−32.2 (4.1)	n/d
Fe^{2+}	−12.5 (1.8)	−11.8 (2.0)	−11.5 (0.6)	−9.5 (3.1)	−13.1 (1.6)	−11.6 (5.7)	−1.2 (0.7)
C (Scotch College)							
Nitrate	−33.7 (0.5)	−46.2 (2.3)*	−48.3 (1.3)	−50.4 (6.7)	n/d	n/d	n/d
Nitrite	15.4 (0.6)	15.7 (0.8)	−1.5 (0.2)†	−1.0 (0.1)†	−26.6 (1.1)*	−22.6 (1.2)	n/d
Fe^{2+}	−14.9 (1.8)	−25.5 (4.0)	−8.5 (0.3)	−21.2 (5.8)	−11.7 (2.6)	−19.7 (2.0)	−5.1 (2.6)
D (Morell Bridge)							
Nitrate	−15.2 (0.7)	−16.4 (1.1)	−29.8 (1.5)	−26.4 (1.3)	n/d	n/d	n/d
Nitrite	4.1 (0.3)	4.6 (1.1)	−0.9 (3.8)†	2.4 (0.1)†	−18.7 (2.7)	−21.0 (1.2)	n/d
Fe^{2+}	−7.2 (0.4)	−11.1 (1.2)	−6.5 (1.3)	−14.0 (1.4)	−5.9 (0.3)	−10.1 (1.4)	−0.6 (0.8)
E (Bay)							
Nitrate	−8.8 (1.1)	−14.8 (3.9)	−27.4 (0.3)	−27.8 (2.0)	n/d	n/d	n/d
Nitrite	3.1 (0.1)	6.2 (1.8)	0.0 (0.0)†	−1.6 (0.1) †	−6.9 (1.1)	−11.1 (0.0)*	n/d
Fe^{2+}	0.0 (0.0)	−5.9 (1.7)	0.7 (0.3)	−4.2 (0.5)	0.0 (0.0)	−3.8 (1.0)	−3.1 (0.7)

entirely removed before the end of the time series (~1 week) at sites A, B, and C, while some nitrate persisted at sites D and E (example in Fig. 3). Nitrite accumulated during nitrate consumption at all sites, with initial accumulation rates accounting for up to half of the nitrate consumption, and net consumption only began once nitrate was depleted at sites A, B, and C.

At all sites, ^{15}N-N$_2$ increased linearly while nitrate and/or nitrite was present in slurries. Accumulation ceased in the cases when nitrate and nitrite were fully depleted (example in Fig. 3). Likewise, ^{15}NH$_4^+$ increased linearly at all sites, ceasing if nitrate and nitrite were fully consumed. While concentrations of dissolved Fe^{2+} were stable during the preincubation before addition of ^{15}N-labeled substrate (Fig. 3), active

Table 4. Partitioning of iron(II) between dissolved (0.2 μm filterable) and particulate phases of samples with sulfamic acid from slurry experiments with ^{15}N-nitrate (+/− Fe^{2+}). (SD) $n = 3$.

| Site | Treatment | Average initial Fe^{2+} (μmol L^{-1}) | | Average Fe^{2+} addition (μmol L^{-1}) |
		Filterable	Particle associated	
A	Control	4.2 (1.6)	179 (18)	
	+ Fe^{2+}	8.5 (0.4)	665 (28)	491
B	Control	34.2 (5.3)	581 (131)	
	+ Fe^{2+}	41.8 (1.0)	1117 (85)	544
C	Control	56.5 (3.4)	367 (13)	
	+ Fe^{2+}	91.0 (15.7)	817 (100)	485
D	Control	39.4 (1.5)	384 (108)	
	+ Fe^{2+}	58.7 (9.5)	979 (35)	614
E	Control	0.1 (0.2)	347 (310)	
	+ Fe^{2+}	33.4 (9.9)	968 (4)	654

removal of dissolved Fe^{2+} was observed immediately following substrate addition and Fe^{2+} removal was significantly higher than in control slurries with no ^{15}N-substrate (significant differences here and hereafter are determined from *t*-tests at 5% confidence level; see Methods section).

In slurries with ^{15}N-nitrate only, rates of nitrate consumption varied greatly between sites, ranging from 8.8 μmol L slurry^{-1} d^{-1} to 35.4 μmol L slurry^{-1} d^{-1} at sites E and B, respectively (Fig. 4; Table 3). Nitrite and N$_2$ were the dominant products of nitrate reduction in experiments with only ^{15}N-nitrate addition; the two accumulating at comparable rates at all sites and contributing >90% of the recovered ^{15}N products (Fig. 4). Accordingly, denitrification dominated over reduction to ammonium as sink for nitrate + nitrite, accounting for >78% of NO$_x^-$ reduction at all sites. Highest rates of ^{15}N-N$_2$ accumulation were observed at site B (14 μmol L slurry^{-1} d^{-1}) while the highest rate of ^{15}NH$_4^+$ production was at site C (2.4 μmol L slurry^{-1} d^{-1}). The highest rates of Fe^{2+} consumption on addition of ^{15}N-nitrate to slurries were observed at sites B, C, and D (ranging from 7.2 μmol Fe^{2+} L slurry^{-1} d^{-1} to 14.9 μmol Fe^{2+} L slurry^{-1} d^{-1}), while rates were low (0–1 μmol Fe^{2+} L slurry^{-1} d^{-1}) in slurries with sediments from site A and E (Fig. 4); potentially being limited by the low background Fe^{2+} concentrations (Table 4).

One set of slurry vials were amended with ^{15}N-nitrite to determine whether nitrate or nitrite reduction was most critical in influencing the fate of nitrogen compounds. Rates of nitrite reduction were not significantly different from nitrate reduction rates in parallel experiments with added ^{15}N-nitrate at sites C, D, and E. At sites A and B, nitrite reduction was significantly slower than nitrate reduction, by approximately 20% and 50%, respectively (Table 3). Accumulation of ^{15}N-N$_2$ increased marginally relative to slurries with ^{15}N-nitrite but the difference was not significant. Ammonium production was also not significantly altered by nitrite as

opposed to nitrate addition except at sites B and C where ^{15}NH$_4^+$ production increased significantly. Significant differences in Fe^{2+} removal rates between ^{15}N-nitrate and -nitrite incubations were only observed at site B, where ^{15}N-nitrite addition reduced Fe^{2+} removal by ∼20%.

The addition of acetate to ^{15}N-nitrate incubations increased rates of nitrate reduction and N$_2$ production at all sites (Table 3; Fig. 5) compared with slurries amended with only ^{15}N-nitrate. In these experiments, nitrate was typically depleted within 2 d of the acetate addition, while nitrite build-up was either markedly reduced or not observed at all (Fig. 5). Accumulation of ^{15}NH$_4^+$ was unaffected by acetate at sites B, C, and D, while it increased slightly at site A and substantially at the site E. The initial linear decrease in Fe^{2+} was not significantly different to vials with ^{15}N-nitrate at sites A, B, and D, but was slowed significantly by acetate addition at site C. At all sites, after all nitrate and nitrite had been removed in acetate-amended slurries, production of ^{15}N-N$_2$ and ^{15}NH$_4^+$ ceased and concentrations of dissolved Fe^{2+} began to increase, indicating that remaining acetate was utilized as a substrate for heterotrophic Fe(III) reduction.

Addition of Fe^{2+} to slurry experiments

Due to the binding of Fe^{2+} to particles mentioned previously, the addition of Fe^{2+} resulted in increases in the final dissolved (0.2 μm filterable) Fe^{2+} concentration of 4–34 μmol L^{-1} corresponding to only 1–7% of the amount added, while the remainder could be recovered by extraction from the solids (Table 4).

Addition of Fe^{2+} to slurry incubations with ^{15}N-nitrate enhanced mean nitrate reduction rates at all sites (Table 3). The observed stimulation of nitrate reduction was deemed significant at sites A, B, and C with enhancements of 38%, 18%, and 37%, respectively (Fig. 4). Stimulation of nitrate reduction by Fe^{2+} addition in the site E was significant at the 10% level ($p = 0.06$, *t*-test) compared with control vials.
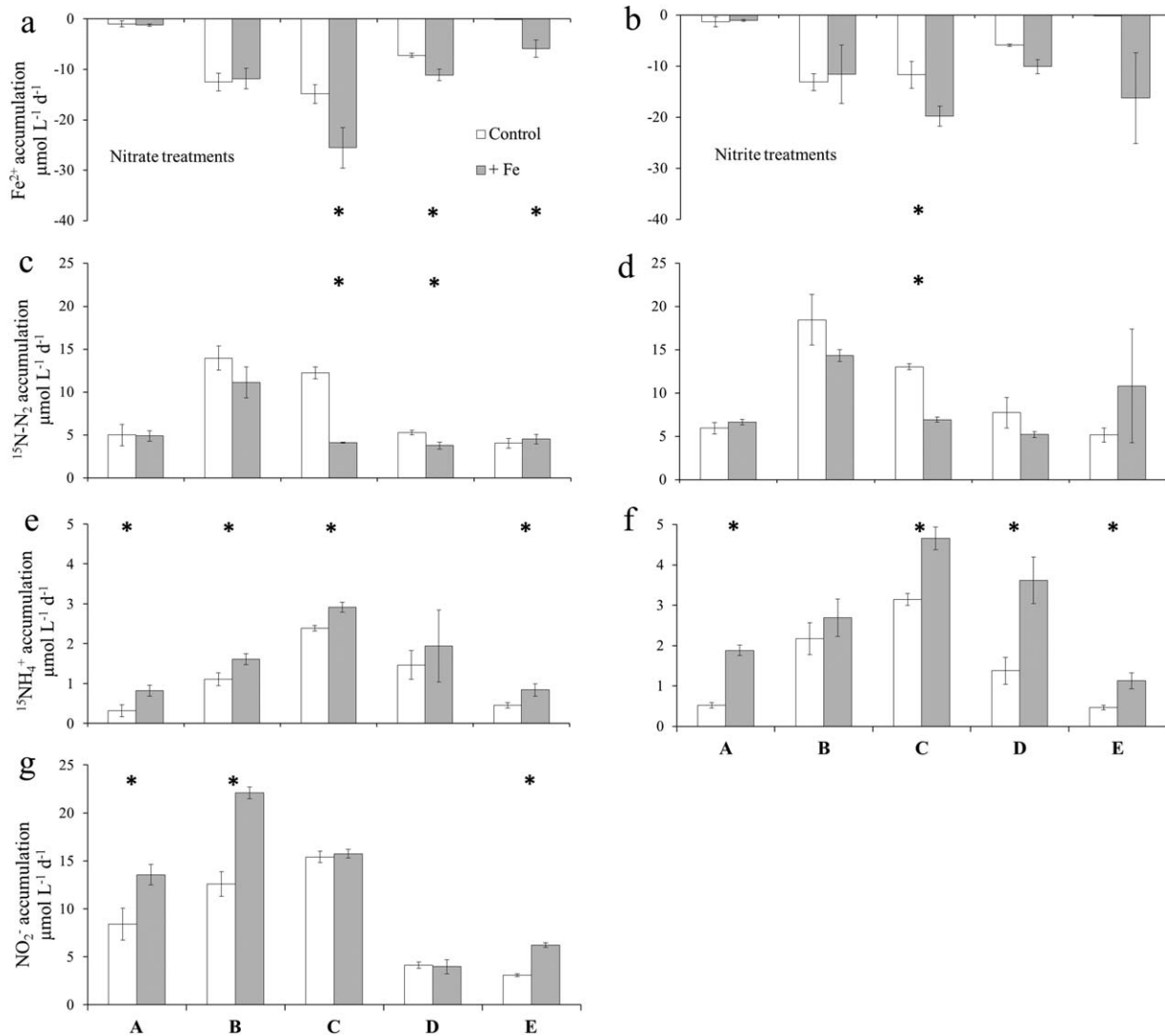
Fig. 4. Average rates of Fe^{2+} consumption (**a, b**) and $^{15}N\text{-}N_2$ (**c, d**), $^{15}NH_4^+$ (**e, f**) production and NO_2^- accumulation (**g**) rates from dilute slurry experiments (μmol N or Fe^{2+} L slurry^{-1} d^{-1}). Asterisks (*) above bars show significant ($p > 0.05$, t-test) differences between control and iron-amended slurries. Bars show SD ($n = 3$).

In incubations with ^{15}N-nitrate, rates of nitrite accumulation tended to increase with Fe^{2+} addition relative to controls, with significant increases in nitrite production rates observed at sites A, B, and E (increases of approximately 77%, 70%, and 100%, respectively; Fig. 4; Table 3). The addition of Fe^{2+} also increased the rate of ^{15}N-ammonium production across all sites relative to control slurries (Fig. 4) with significant enhancement observed at all but site D. By contrast, production of $^{15}N\text{-}N_2$ was significantly reduced by Fe^{2+} addition at sites C and D, while it was not affected at the other sites. The rate of Fe^{2+} consumption was significantly enhanced at sites C and D as well as at site E, however this was relative to low background Fe^{2+} in control incubations (Fig. 4).

Similarly to the ^{15}N-nitrate slurries, addition of Fe^{2+} to slurries with ^{15}N-nitrite increased rates of nitrite consumption at all sites except site C, where a decrease in nitrite reduction in response to Fe^{2+} addition was observed (Table 3). Significant stimulations in nitrite consumption were recorded at sites A and E. Addition of Fe^{2+} to ^{15}N-nitrite slurries stimulated ^{15}N-ammonium production at all sites except site D (Fig. 3; Table 3). Production of $^{15}N\text{-}N_2$ from ^{15}N-nitrite was enhanced slightly, although not significantly, by Fe^{2+} compared with controls at sites A and E, whereas $^{15}N\text{-}N_2$ production decreased in response to Fe^{2+} addition at sites B, C, and D (Fig. 3; Table 3). In these incubations, rates of Fe^{2+} removal in slurries was enhanced at all sites except site A where rates remained unchanged (Fig. 3; Table 3).
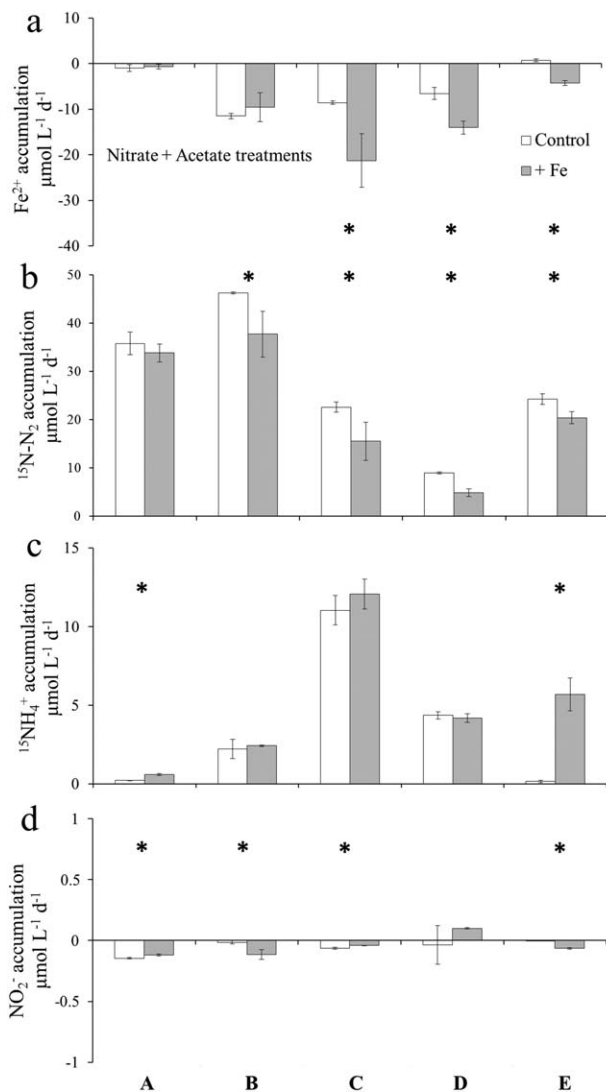
Fig. 5. Average rates of Fe^{2+} consumption (**a**), $^{15}N\text{-}N_2$ (**b**), $^{15}NH_4^+$ (**c**) production and NO_2^- accumulation (**d**) rates from dilute slurry experiments (μmol N or Fe^{2+} L slurry^{-1} d^{-1}) with ^{15}N-nitrate and acetate additions. Negative values of NO_2^- accumulation are due to an initial small accumulation followed by rapid depletion. Asterisks (*) above bars show significant ($p > 0.05$, t-test) differences between control and iron-amended slurries. Bars show SD ($n = 3$).

The alteration in the dominant nitrate reduction process after Fe^{2+} amendment is further illustrated by the shift in the ratio of N_2 production to ammonium production (denitrification: DNRA; Table 5). This ratio decreased consistently after the addition of Fe^{2+} in both nitrate and nitrite incubations.

The rate of Fe^{2+} removal was significantly correlated ($p < 0.05$, F-test) with the production of $^{15}NH_4^+$ in data compiled from all slurries (Fig. 6). The slopes of the linear regressions of NO_x reduction to ammonium vs. Fe^{2+} consumption were 0.10 and 0.19 for nitrate and nitrite respectively, corresponding to stoichiometries of Fe^{2+} oxidation with ammonium production of 1: 10.0 and 1: 5.3 for ^{15}N-nitrate and ^{15}N-

Table 5. Average ratios of denitrification to DNRA in slurry experiments with ^{15}N-substrates in comparison to those with added Fe^{2+}. (SD) $n = 3$.

	Denitrification: DNRA			
	^{15}N-nitrate	^{15}N-nitrate + Fe^{2+}	^{15}N-nitrite	^{15}N-nitrite + Fe^{2+}
A	18.4 (7.3)	6.2 (1.6)	11.6 (2.4)	3.5 (0.2)
B	12.9 (2.5)	6.9 (0.7)	8.5 (0.5)	5.5 (1.1)
C	5.1 (0.4)	1.4 (0.1)	4.2 (0.1)	1.5 (0.6)
D	3.8 (1.0)	2.3 (0.1)	6.1 (3.2)	1.5 (0.3)
E	9.0 (0.4)	5.6 (1.2)	11.3 (3.1)	9.3 (4.2)

nitrite experiments, respectively. There was no correlation between Fe^{2+} consumption and denitrification rates across all incubations with either nitrate or nitrite (Fig. 6).

A plot of ammonium accumulation rates vs. initial soluble Fe^{2+} concentrations indicated a Michaelis–Menten-type rate dependence, with a maximum reaction rate of 8.1 ± 3.3 μmol L^{-1} d^{-1} and a half saturation constant of 122.0 ± 72.6 μmol Fe^{2+} L^{-1} obtained from a non-linear least-squares fit (Fig. 7).

The combined addition of Fe^{2+} and acetate to ^{15}N-nitrate slurries (Table 3; Fig. 5) caused significant reductions in ^{15}N-N_2 production relative to incubations with acetate and ^{15}N-nitrate only at all sites except at site A. At this site, $^{15}NH_4^+$ production increased significantly relative to slurries without additional Fe^{2+}, while no significant increases in $^{15}NH_4^+$ production were observed at the remaining four sites. A buildup of nitrite was enhanced in vials with added Fe^{2+} at all sampling sites (Fig. 3), however the concentration to which nitrite accumulated varied greatly between each site (data not shown). Removal of Fe^{2+} was significantly enhanced relative to slurries with only acetate and ^{15}N-nitrate at site C, D, and E, whereas no significant changes were observed at sites A and B. At site E this enhancement was most likely due to there being very low background Fe^{2+}.

Discussion

Iron-fueled nitrate reduction

Our experiments demonstrate clear and consistent effects of Fe^{2+} on the reductive transformations of both nitrate and nitrite in aquatic sediments across a transition from freshwater to seawater. Furthermore, we show a stoichiometric coupling of Fe^{2+} oxidation and nitrate/nitrite reduction to ammonium in sediment under environmentally relevant substrate concentrations. Our results point primarily to a microbially mediated, dissimilatory process rather than an abiotic pathway, as discussed in detail below. We therefore use the term DNRA for the observed nitrate and nitrite reduction to ammonium throughout this discussion. The experiments permit quantitative estimates of the contribution of Fe^{2+} oxidation to DNRA
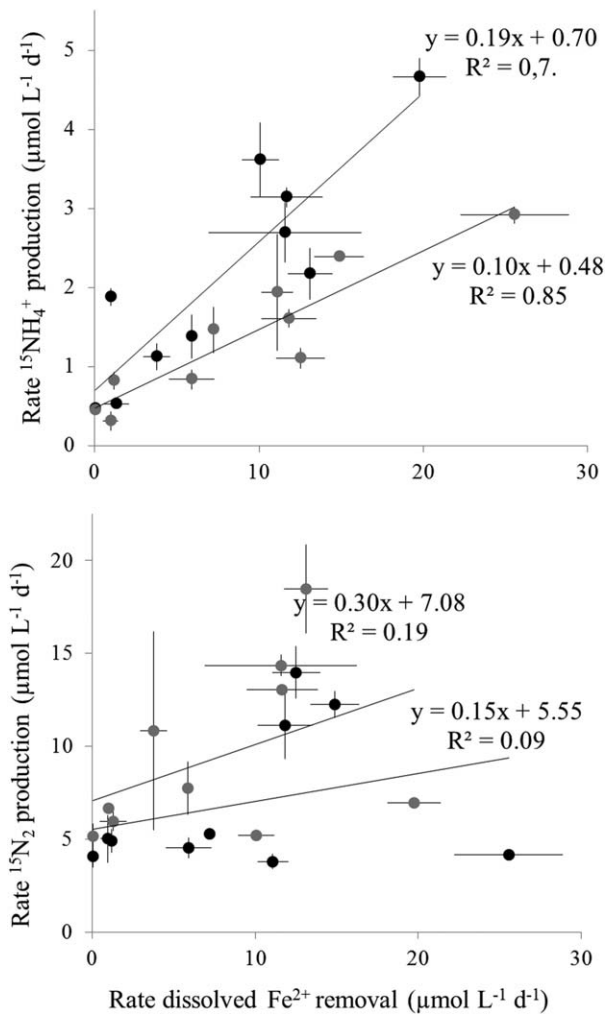
Fig. 6. Correlation between average rates of Fe^{2+} removal and $^{15}NH_4^+$ production (top panel) and ^{15}N-N_2 production (bottom panel) in slurry incubations with ^{15}N-nitrate (black dots) and ^{15}N-nitrite additions (grey dots) from all sites investigated. No rates are included from experiments with ^{15}N-nitrate and acetate addition.

and nitrogen cycling across the estuarine gradient. Our results suggest that Fe^{2+} is an important electron donor for DNRA in the Yarra River estuary, and that variations in Fe^{2+} availability are likely to be playing a key role in regulating the fate of bio-available nitrogen.

Rates of NO_x reduction to ammonium were stimulated significantly by addition of Fe^{2+} in 8 of 10 experiments, while rates of N_2 production were either unchanged or decreased (Fig. 4). This shift in the dominant nitrate reduction process is further expressed in the relative contribution of DNRA to nitrate + nitrite reduction, which increased markedly from 10–20% to almost 50% with the addition of Fe^{2+}, greatly altering denitrification: DNRA ratios (Table 5). This shift is in line with a previous study where similar alterations in denitrification: DNRA ratio were observed and linked to changes between the dominance of Fe^{2+} and sul-
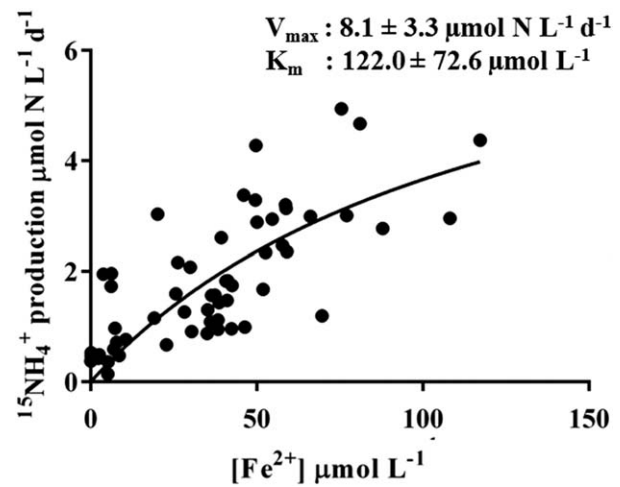

Fig. 7. Michaelis Menten kinetics of DNRA rate (as $^{15}NH_4^+$ production) against the initial Fe^{2+} concentration in all slurry experiments (excluding those with acetate addition) $\pm$ SD.

fide in porewaters under oxic and hypoxic conditions, respectively (Roberts et al. 2014). In addition, the correlation of DNRA rates to rates of Fe^{2+} consumption, and the similarity of stoichiometries to those expected for Fe^{2+}-based DNRA (Table 1; Fig. 6) strongly support a direct coupling of the processes. Thus, in experiments with ^{15}N nitrite, the regression-based ratio of Fe^{2+} oxidation to DNRA was 5.3, which is very close to the predicted stoichiometry of 6 (Table 1). With ^{15}N-nitrate, the observed ratio was somewhat higher than predicted (10.0 rather than 8). This is likely because part of the Fe^{2+} oxidation was coupled to the net production of nitrite by nitrate reduction, which was also stimulated by Fe^{2+} addition in some experiments (Fig. 4). Thus, our results imply that Fe^{2+} oxidation is coupled to both reduction steps involved in DNRA ($NO_3^- \rightarrow NO_2^-$ and $NO_2^- \rightarrow NH_4^+$; Table 1). Furthermore, the low, positive y-intercept of linear regressions indicates that a small proportion of DNRA (~ 0.5 μmol N L slurry^{-1} d^{-1}; Fig. 6) may proceed without Fe^{2+}. This suggests some DNRA may be independent of Fe^{2+} oxidation and is instead coupled to oxidation of an organic substrate, but also that most of the DNRA at the sites with high Fe^{2+} concentrations in the pore waters, where DNRA is most active (Figs. 3, 4), is coupled to Fe^{2+} oxidation. In contrast, we observed no evidence for a coupling of denitrification to Fe^{2+} oxidation and increasing Fe^{2+} concentrations even partially inhibited this process at some sites.

While Fe^{2+}-based NO_x reduction in the slurries may be microbially catalyzed, we cannot completely exclude an involvement of abiotic reactions. As Fe(II) in green rusts (GR) shows particularly high reactivity toward nitrate we estimated potential rates of abiotic nitrate reduction, applying rate expressions from a previous study (Hansen et al. 1996), rate constants for chloride GR (GR_{Cl}) or sulfate GR (GR_{SO_4}) (Hansen et al. 2001) and our own initial nitrate and

particle-associated Fe(II) concentrations from slurry experiments ($\sim$100 μmol L^{-1} nitrate and $\sim$500–1000 μmol L^{-1} Fe(II); Table 4). Based on these calculations, abiotic reduction of nitrate to ammonium could potentially account for $\sim$1–4 or $\sim$0.04–0.1 μmol NH$_4^+$ L^{-1} d^{-1} for GR$_{Cl}$ or GR$_{SO_4}$, respectively. However these values are most likely overestimates as this assumes that all Fe^{2+} measured in slurries is in the form of GR$_{Cl}$ or GR$_{SO_4}$. While this suggests that abiotic reactions could account for some of the observed enhancements of nitrate reduction to ammonium, we further suggest that the observed accumulation of nitrite in slurries indicates a biotic mechanism for at least part of the nitrate reduction observed. Nitrite accumulation is a normal phenomenon during microbial denitrification and DNRA, resulting from differences in kinetics between enzymes (Betlach and Tiedje 1981). By contrast, nitrite is abiotically more reactive than nitrate and well known to undergo abiotic reactions in the presence of Fe^{2+} (Hansen et al. 1994; Tai and Dempsey 2009; Klueglein and Kappler 2013), while we observed enhanced nitrite accumulation with increased Fe^{2+} availability in some cases. Nitrite accumulation would be expected to decrease at increasing Fe^{2+} concentrations, should abiotic reactions have been occurring. We also observed no blue-green color of sediment in slurry experiments which may indicate the presence of GR formation (Hansen et al. 1994). While it is difficult to conclusively discern abiotic vs. biotic reactions given discrepancies in reaction rate constants in the literature (Hansen et al. 1996; Etique et al. 2014), we suggest our results to be indicative of microbially mediated dissimilatory processes, which implies that it is appropriate to refer to the measured ^{15}NH$_4^+$ accumulation as DNRA.

Addition of acetate to slurries provided further insight into the nature of microbially mediated nitrate reduction processes in Yarra River sediment. The large, immediate stimulation of ^{15}N-N$_2$ production and lack of nitrite accumulation observed in slurries with acetate addition (Table 3; Fig. 5) indicates the heterotrophic potential of denitrification. This, together with the lacking or negative effect of Fe^{2+} addition on this process, suggests that denitrification is predominantly a heterotrophic process, which was limited by organic substrate at least under slurry conditions. Rates of ^{15}NH$_4^+$ accumulation in incubations with acetate were equal to those in ^{15}N-nitrate experiments or slightly increased (Table 3), suggesting that acetate was generally not a limiting factor for DNRA. Slight increases may be explained by a proportion of the community carrying out DNRA with an organic substrate as opposed to Fe^{2+} (as discussed previously). The addition of acetate also had no discernable effect on rates of Fe^{2+} consumption. Thus, the acetate addition experiments suggest that Fe^{2+}-fueled NO$_x$ reduction may be a purely chemolithotrophic and possibly autotrophic process in the Yarra River. Although autotrophic nitrate-reducing iron-oxidizing strains have been isolated (Vorholt et al. 1997; Weber et al. 2006a; Li et al. 2014), most known strains

carrying out this process employ a mixotrophic (mixed litho- and organotrophic) metabolism where an organic co-substrate such as acetate is also oxidized during growth (e.g., Straub et al. 1996; Benz et al. 1998; Chakraborty and Picardal 2013b). If this were the case in our slurries, we would expect a stimulation of Fe^{2+} oxidation by acetate addition.

While this study shows that Fe^{2+} oxidation is linked to DNRA, studies of bacterial cultures have predominantly shown Fe^{2+} oxidation to be coupled to denitrification (e.g., Straub et al. 1996; Weber et al. 2001; Kappler et al. 2005). This suggests that the conditions used for cultivation, typically including millimolar substrate concentrations, select for different anaerobic iron oxidizers than those that are most active in the sediments. High substrate concentrations also appear to cause the encrustation and thereby inhibition of nitrate-dependent Fe^{2+} oxidizers by Fe(III) minerals (Kappler et al. 2005; Chakraborty and Picardal 2013b; Klueglein et al. 2014), whereas growth of *Acidovorax* strain 2AN at environmental substrate concentrations (100 μmol L^{-1} nitrate, 20 μmol L^{-1} acetate, 50–250 μmol L^{-1} Fe^{2+}) proceeded without hindrance by mineral formation. Other studies have also reported indirect evidence of an association of N cycling with Fe^{2+} oxidation, with significant correlations of nitrate reducing process rates with Fe oxide content in coastal sediments in the U.S.A. (Hou et al. 2012) and China (Yin et al. 2014). In both studies, Fe^{2+} oxidation was suggested to be linked to denitrification at 100 μmol L^{-1} nitrate, although a significant correlation between DNRA and Fe oxides was also observed in one of the studies (Hou et al. 2012). The capacity for Fe^{2+}-fueled nitrate reduction may thus be widespread under environmental conditions, and high nitrate concentrations typically experienced in enrichment cultures are unlikely to reflect how organisms respond to substrate availability in more complex natural systems.

The exact mechanism for the decrease in denitrification with increased Fe^{2+} concentration cannot be identified in this study. As nitrate and nitrite concentrations were high initially, it does not seem likely that the increased Fe^{2+} availability conferred a competitive advantage to those organisms carrying out Fe^{2+}-driven DNRA. It is possible that higher Fe^{2+} concentrations reduce the rate of heterotrophic denitrification by inhibiting cellular processes via potential toxic reactions of Fe^{2+} in cells (Carlson et al. 2012 and references therein). In this way, organisms carrying out Fe^{2+}-fueled DNRA may gain advantage over heterotrophic denitrifiers when exposed to high Fe^{2+} concentrations in situ. Both nitrate and nitrite were already depleted in the upper few millimeters of the sediment where pore water Fe^{2+} concentrations were $\geq$ 100 μmol L^{-1} at three sites. Comparatively, Fe^{2+} concentrations in our slurries were typically $<$ 100 μmol L slurry^{-1} (Table 4), which suggests the potential for this process may be even greater in situ. Reaction kinetics of DNRA relative to Fe^{2+} concentration with an apparent K_m of 122 μmol Fe^{2+} L^{-1} (Fig. 7) substantiated the potential for

higher rates. Thus, further considering the possible inhibitory effect of Fe^{2+} on denitrification, it is possible the DNRA may be the dominant nitrate reducing process in the environment as observed by Roberts et al. (2014) in these sediments while the overlying water column was oxic. As such, Fe^{2+}-fueled NO_x reduction could significantly influence the fate of nitrate introduced to the Yarra River depending on Fe^{2+} availability.

Environmental implications

Slurry experiments performed here provide important mechanistic insight into the factors controlling DNRA and help explain previous observations of DNRA in intact core incubations within the Yarra Estuary (Roberts et al. 2012, 2014). While the slurrying of sediments may have associated caveats related to the removal of geochemical gradients and sediment homogenization (e.g., Hansen et al. 2000), they also provide invaluable information on controls on biogeochemical processes. Nitrogen cycling in particular is challenging to investigate in intact sediment cores where processes are typically restricted to a narrow depth horizon. In this study, slurries allowed process rates to be more easily controlled, manipulated and compared between different sediment types; providing important information on the links between iron and nitrogen cycles.

In dynamic estuarine environments, variation in freshwater and marine inputs can cause substantial alterations from diurnal (e.g., tidal cycles) to seasonal (changes in freshwater flow) timescales. As such, dissolved components such as nutrients can vary widely in the same river depending on water flow (Cabrita and Brotas 2000; Dong et al. 2011). In the Yarra River, interannual changes in the contribution of denitrification and DNRA have been previously determined at three of the five sites investigated here (Roberts et al. 2012). We found concentrations of dissolved pore water constituents, nutrient fluxes and whole core denitrification rates presented here are comparable to those measured in previous studies on the Yarra River during austral summer months (Roberts et al. 2012, 2014). Therefore we suggest that the conditions at the time of sampling were representative of the geochemical regime of the Yarra River during the austral summer.

Nutrient concentrations in both sediments and overlying water measured in this study are also comparable to those reported in other temperate estuaries (e.g., Hopkinson et al. 1999; Cabrita and Brotas 2000; Crowe et al. 2012). In addition, high sediment Fe contents are also known to occur through deposition at the mouths of major river systems such as the Amazon and Mississippi (Aller et al. 1986; Powell and Wilson-Finelli 2003), where high Fe reduction rates can lead to comparable concentrations of dissolved Fe in the upper centimeters of sediment (Aller et al. 1986). Thus the geochemical condition of the Yarra River estuary is comparable to other estuarine sites, suggesting the findings of this study may be more widely applicable to other systems.

Previous work on the Yarra River observed a reduction of both DNRA and denitrification under hypoxia and indicated that DNRA may be inhibited to a greater extent than denitrification under low oxygen conditions (Roberts et al. 2012). In contrast, increases in DNRA are commonly reported under reducing conditions such as during periods of low water column oxygen concentrations or incidences of high carbon loading in other sediments (Christensen et al. 2000; An and Gardner 2002; Jäntti and Hietanen 2012). In a subsequent study on the Yarra River, it was suggested that the observed alterations may be linked to fluctuations in Fe^{2+} availability (Roberts et al. 2014), however a clear link was not found in slurry experiments with Fe^{2+} additions. The binding of free Fe^{2+} by sulfide produced under low oxygen regimes was suggested to be a major controlling factor as to why DNRA was observed to decrease so markedly (Roberts et al. 2014). This study confirms the hypothesis of Roberts et al. (2014) in that changes in Fe^{2+} availability altered the relative importance of N cycling processes, leading to recycling of N in sediments although increased DNRA.

Depth profiles and in situ parameters reported here reveal the wide variation in both sediment and water chemistry between sites at the time of sampling and are likely to cause the differences in the potential for Fe^{2+}-driven DNRA along the estuarine gradient. The reduction of sulfate introduced from seawater intrusion, and subsequent production of sulfide, exerts strong control on Fe^{2+} availability; with sulfide binding rapidly with Fe^{2+} to form solid iron sulfides. The presence of microorganisms adapted to higher Fe^{2+} availability available in surface (upper 0.5–1 cm) sediment in the three sites with least marine influence (A, B, and C) may go some way to explaining the stimulation of Fe^{2+}-driven DNRA. While stimulation of DNRA by Fe^{2+} addition was also observed at sites D and E under slurry conditions, the production of sulfide (detected only at site D) may reduce available Fe^{2+} concentrations by the formation of iron sulfides, thus reducing the potential for Fe^{2+}-fueled DNRA in situ.

An additional factor that may increase the availability of Fe^{2+} in periodically hypoxic estuaries is the presence of filamentous "cable" bacteria of the *Desulfobulbaceae* (Pfeffer et al. 2012). These organisms couple spatially separated biogeochemical processes, with anoxic sulfide oxidation leading to significant decreases in sediment pH (Pfeffer et al. 2012) and causing the liberation of Fe^{2+} by the subsequent dissolution of FeS (Risgaard-Petersen et al. 2012). Consistent with this, we have observed the rapid growth of these filamentous bacteria in repacked sediment cores from our study sites, with the subsequent liberation of ~ 1 mmol L^{-1} Fe^{2+} in the top 5 mm of sediment within 7 d (L. Burdorf pers. comm.). These observations are also consistent with the rapid onset of DNRA in re-oxygenated cores previously observed in these sediments (Roberts et al. 2014).

This study is to our knowledge the first to have demonstrated and quantified Fe^{2+}-dependent DNRA under

environmentally relevant conditions. Previous sediment studies have mainly linked DNRA to low redox potential and the oxidation of sulfide and other reduced sulfur compounds (Christensen et al. 2000; An and Gardner 2002; Jäntti and Hietanen 2012), and specifically to the presence of the filamentous sulfur bacteria *Beggiatoa* and *Thioploca* that perform sulfide-dependent DNRA (Otte et al. 1999; Schulz and Jørgensen 2001; Sayama et al. 2005). Fe^{2+} dependent DNRA was previously demonstrated in first-cycle enrichments of sediments from a freshwater wetland and a river, suggesting that the process may also be important there (Weber et al. 2006b; Coby et al. 2011). We speculate that the process may be of general importance for nitrate reduction in sediments with a high Fe^{2+} availability such as estuaries, where iron-rich catchment-derived colloidal material undergoes coagulation and settling (Ellaway et al. 1980). Thus, the process could potentially contribute to the dominance of DNRA over denitrification reported for tropical estuaries (Dong et al. 2011) considering the typically high particulate iron load of tropical rivers (Martin and Meybeck 1979). The contribution of Fe^{2+}-driven processes to sediment nitrate reduction may thus be an important factor in determining whether introduced N is removed or retained in these environments; and as such affect the important role of estuarine and coastal sediments as sinks for anthropogenic nitrogen from land (Seitzinger et al. 2006).

References

Aller, R. C., J. E. Mackin, and R. T. Cox. 1986. Diagenesis of Fe and S in Amazon inner shelf muds: Apparent dominance of Fe reduction and implications for the genesis of ironstones. Cont. Shelf Res. **6**: 263–289. doi:10.1016/0278-4343(86)90064-6

An, S., and W. Gardner. 2002. Dissimilatory nitrate reduction to ammonium (DNRA) as a nitrogen link, versus denitrification as a sink in a shallow estuary (Laguna Madre/Baffin Bay, Texas). Mar. Ecol. Prog. Ser. **237**: 41–50. doi:10.3354/meps237041

Benz, M., A. Brune, and B. Schink. 1998. Anaerobic and aerobic oxidation of ferrous iron at neutral pH by chemoheterotrophic nitrate-reducing bacteria. Arch. Microbiol. **169**: 159–65. doi:10.1007/s002030050555

Betlach, M. R., and J. M. Tiedje. 1981. Kinetic explanation for accumulation of nitrite, nitric oxide, and nitrous oxide during bacterial denitrification. Appl. Environ. Microbiol. **42**: 1074–1084.

Boynton, W. R., and W. M. Kemp. 2008. Estuaries, p. 809–866. *In* D. Capone, D. Bronk, M. Mulholland, and E. Carpenter [eds.], Nitrogen in the marine environment. Academic Press.

Brettar, I., and G. Rheinheimer. 1992. Influence of carbon availability on denitrification in the central Baltic Sea. Limnol. Oceanogr. **37**: 1146–1163. doi:10.4319/lo.1992.37.6.1146

Brunet, R. C., and L. J. Garcia-Gil. 1996. Sulfide-induced dissimilatory nitrate reduction to ammonia in anaerobic freshwater sediments. FEMS Microbiol. Ecol. **21**: 131–138. doi:10.1111/j.1574-6941.1996.tb00340.x

Burgin, A. J., and S. K. Hamilton. 2007. Have we overemphasized the role of denitrification in aquatic ecosystems? A review of nitrate removal pathways. Front. Ecol. Environ. **5**: 89–96. doi:10.1890/1540-9295(2007)5[89:HWOTRO]2.0.CO;2

Cabrita, M., and V. Brotas. 2000. Seasonal variation in denitrification and dissolved nitrogen fluxes in intertidal sediments of the Tagus estuary, Portugal. Mar. Ecol. Prog. Ser. **202**: 51–65. doi:10.3354/meps202051

Carlson, H. K., I. C. Clark, R. A. Melnyk, and J. D. Coates. 2012. Toward a mechanistic understanding of anaerobic nitrate-dependent iron oxidation: Balancing electron uptake and detoxification. Front. Microbiol. **3**: 57. doi:10.3389/fmicb.2012.00057

Carlson, H. K., I. C. Clark, S. J. Blazewicz, A. T. Iavarone, and J. D. Coates. 2013. Fe(II) oxidation is an innate capability of nitrate-reducing bacteria that involves abiotic and biotic reactions. J. Bacteriol. **195**: 3260–3268. doi:10.1128/JB.00058-13

Chakraborty, A., E. E. Roden, J. Schieber, and F. Picardal. 2011. Enhanced growth of *Acidovorax* sp. strain 2AN during nitrate-dependent Fe(II) oxidation in batch and continuous-flow systems. Appl. Environ. Microbiol. **77**: 8548–8556. doi:10.1128/AEM.06214-11

Chakraborty, A., and F. Picardal. 2013a. Induction of nitrate-dependent Fe(II) oxidation by Fe(II) in *Dechloromonas* sp. strain UWNR4 and *Acidovorax* sp. strain 2AN. Appl. Environ. Microbiol. **79**: 748–752. doi:10.1128/AEM.02709-12

Chakraborty, A., and F. Picardal. 2013b. Neutrophilic, nitrate-dependent, Fe(II) oxidation by a *Dechloromonas* species. World J. Microbiol. Biotechnol. **29**: 617–623. doi:10.1007/s11274-012-1217-9

Christensen, P. B., S. Rysgaard, N. P. Sloth, T. Dalsgaard, and S. Schwærter. 2000. Sediment mineralization, nutrient fluxes, denitrification and dissimilatory nitrate reduction to ammonium in an estuarine fjord with sea cage trout farms. Aquat. Microb. Ecol. **21**: 73–84. doi:10.3354/ame021073

Cline, J. D. 1969. Spectrophotometric determination of hydrogen sulfide in natural waters. Limnol. Oceanogr. **14**: 454–458. doi:10.4319/lo.1969.14.3.0454

Coby, A. J., and F. W. Picardal. 2005. Inhibition of NO3− and NO2− reduction by microbial Fe (III) reduction : Evidence of a reaction between NO2− and cell surface-bound Fe2+. Appl. Environ. Microbiol. **71**: 5267–5274. doi:10.1128/AEM.71.9.5267-5274.2005

Coby, A. J., F. Picardal, E. Shelobolina, H. Xu, and E. E. Roden. 2011. Repeated anaerobic microbial redox cycling of iron. Appl. Environ. Microbiol. **77**: 6036–6042. doi:10.1128/AEM.00276-11

Crowe, S. A., D. E. Canfield, A. Mucci, B. Sundby, and R. Maranger. 2012. Anammox, denitrification and fixed-nitrogen removal in sediments from the Lower St. Lawrence Estuary. Biogeosciences **9**: 4309–4321. doi:10.5194/bg-9-4309-2012

Dalsgaard, T., and others. 2000. Protocol handbook for nitrogen cycling in estuaries: A project under the EU research programme: Marine Science and Technology (MAST III), Ministry of Environment and Energy, National Environmental Research Institute, Department of Lake and Estuarine Ecology, Denmark.

Dhakal, P., C. J. Matocha, F. E. Huggins, and M. M. Vandiviere. 2013. Nitrite reactivity with magnetite. Environ. Sci. Technol. **47**: 6206–6213. doi:10.1021/es304011w

Dong, L. F., and others. 2011. Dissimilatory reduction of nitrate to ammonium, not denitrification or anammox, dominates benthic nitrate reduction in tropical estuaries. Limnol. Oceanogr. **56**: 279–291. doi:10.4319/lo.2011.56.1.0279

Dunn, R. J. K., D. Robertson, P. R. Teasdale, N. J. Waltham, and D. T. Welsh. 2013. Benthic metabolism and nitrogen dynamics in an urbanised tidal creek: Domination of DNRA over denitrification as a nitrate reduction pathway. Estuar. Coast. Shelf Sci. **131**: 271–281. doi:10.1016/j.ecss.2013.06.027

Ellaway, M., R. Beckett, and B. T. Hart. 1980. Behaviour of iron and manganese in the Yarra estuary. Aust. J. Mar. Freshw. Res. **31**: 597–609. doi:10.1071/MF9800597

Etique, M., F. P. A. Jorand, A. Zegeye, B. Grégoire, C. Despas, and C. Ruby. 2014. Abiotic process for Fe(II) oxidation and green rust mineralization driven by a heterotrophic nitrate reducing bacteria (*Klebsiella mobilis*). Environ. Sci. Technol. **48**: 3742–3751. doi:10.1021/es403358v

Giblin, A. E., C. R. Tobias, B. Song, N. Weston, G. T. Banta, and V. H. Rivera-Monroy. 2013. The importance of dissimilatory nitrate reduction to ammonium (DNRA) in the nitrogen cycle of coastal ecosystems. Oceanography **26**: 124–131. doi:10.5670/oceanog.2013.54

Hansen, H. C. B., O. K. Borggaard, and J. Sørensen. 1994. Evaluation of the free energy of formation of Fe(II)-Fe(III) hydroxide-suphate (green rust) and its reduction of nitrite. Geochim. Cosmochim. Acta **58**: 2599–2608. doi:10.1016/0016-7037(94)90131-7

Hansen, H. C. B., C. B. Koch, H. Nancke-Krogh, O. K. Borggaard, and J. Sørensen. 1996. Abiotic nitrate reduction to ammonium: Key role of green rust. Environ. Sci. Technol. **30**: 2053–2056. doi:10.1021/es950844w

Hansen, J. W., B. Thamdrup, and B. B. Jørgensen. 2000. Anoxic incubation of sediment in gas-tight plastic bags: A method for biogeochemical process studies. Mar. Ecol. Prog. Ser. **208**: 273–282. doi:10.3354/meps208273

Hansen, H. C. B., S. Guldberg, M. Erbs, and C. B. Koch. 2001. Kinetics of nitrate reduction by green rusts—effects of interlayer anion and Fe (II) : Fe(III) ratio. Appl. Clay Sci. **18**: 81–91. doi:10.1016/S0169-1317(00)00029-6

Hopkinson, C. S., A. E. Giblin, J. Tucker, and R. H. Garritt. 1999. Benthic metabolism and nutrient cycling along an estuarine salinity gradient. Estuaries **22**: 863–881. doi:10.2307/1353067

Hou, L., M. Liu, S. A. Carini, and W. S. Gardner. 2012. Transformation and fate of nitrate near the sediment–water interface of Copano Bay. Cont. Shelf Res. **35**: 86–94. doi:10.1016/j.csr.2012.01.004

Howarth, R., F. Chan, D. J. Conley, J. Garnier, S. C. Doney, R. Marino, and G. Billen. 2011. Coupled biogeochemical cycles : Eutrophication and hypoxia in temperate estuaries and coastal marine ecosystems. Front. Ecol. Environ. **9**: 18–26. doi:10.1890/100008

Jäntti, H., and S. Hietanen. 2012. The effects of hypoxia on sediment nitrogen cycling in the Baltic Sea. Ambio **41**: 161–169. doi:10.1007/s13280-011-0233-6

Jensen, K. M., and R. P. Cox. 1992. Effects of sulfide and low redox potential on the inhibition of nitrous oxide reduction by acetylene in *Pseudomonas nautica*. FEMS Microbiol. Lett. **96**: 13–18. doi:10.1016/0378-1097(92)90449-X

Kappler, A., B. Schink, and D. K. Newman. 2005. Fe (III) mineral formation and cell encrustation by the nitrate-dependent Fe (II)-oxidizer strain BoFeN1. Geobiology **3**: 235–245. doi:10.1111/j.1472-4669.2006.00056.x

Klueglein, N., and A. Kappler. 2013. Abiotic oxidation of Fe(II) by reactive nitrogen species in cultures of the nitrate-reducing Fe(II) oxidizer *Acidovorax* sp. BoFeN1—questioning the existence of enzymatic Fe(II) oxidation. Geobiology **11**: 180–190. doi:10.1111/gbi.12019

Klueglein, N., F. Zeitvogel, Y.-D. Stierhof, M. Floetenmeyer, K. O. Konhauser, A. Kappler, and M. Obst. 2014. Potential role of nitrite for abiotic Fe(II) oxidation and cell encrustation during nitrate reduction by denitrifying bacteria. Appl. Environ. Microbiol. **80**: 1051–1061. doi:10.1128/AEM.03277-13

Koop-Jakobsen, K., and A. E. Giblin. 2010. The effect of increased nitrate loading on nitrate reduction via denitrification and DNRA in salt marsh sediments. Limnol. Oceanogr. **55**: 789–802. doi:10.4319/lo.2009.55.2.0789

Kraft, B., and others. 2014. The environmental controls that govern the end product of bacterial nitrate respiration. Science. **345**: 676–679. doi:10.1126/science.1254070

Li, B., C. Tian, D. Zhang, and X. Pan. 2014. Anaerobic nitrate-dependent iron (II) oxidation by a novel autotrophic bacterium, *Citrobacter freundii* strain PXL1. Geomicrobiol. J. **31**: 138–144. doi:10.1080/01490451.2013.816393

Martin, J., and M. Meybeck. 1979. Elemental mass-balance of material carried by major world rivers. Mar. Chem. **7**: 173–206. doi:10.1016/0304-4203(79)90039-2

Moraghan, J. T., and R. J. Buresh. 1977. Chemical reduction of nitrite and nitrous oxide by ferrous iron. Soil Sci. Soc. Am. **41**: 47–50. doi:10.2136/sssaj1977.03615995004100010017x

Nizzoli, D., E. Carraro, V. Nigro, and P. Viaroli. 2010. Effect of organic enrichment and thermal regime on denitrification

and dissimilatory nitrate reduction to ammonium (DNRA) in hypolimnetic sediments of two lowland lakes. Water Res. **44**: 2715–2724. doi:10.1016/j.watres.2010.02.002

Otte, S., and others. 1999. Nitrogen, carbon, and sulfur metabolism in natural *Thioploca* samples. Appl. Environ. Microbiol. **65**: 3148–3157.

Ottley, C. J., W. Davison, and W. M. Edmunds. 1997. Chemical catalysis of nitrate reduction by iron (II). Geochim. Cosmochim. Acta **61**: 1819–1828. doi:10.1016/S0016-7037(97)00058-6

Pantke, C., M. Obst, K. Benzerara, G. Morin, G. Ona-nguema, U. Dippon, and A. Kappler. 2012. Green rust formation during Fe(II) oxidation by the nitrate-reducing *Acidovorax* sp. strain BoFeN1. Environ. Sci. Technol. **46**: 1439–1446. doi:10.1021/es2016457

Pfeffer, C., and others. 2012. Filamentous bacteria transport electrons over centimetre distances. Nature **491**: 218–221. doi:10.1038/nature11586

Picardal, F. 2012. Abiotic and microbial interactions during anaerobic transformations of Fe(II) and NOx. Front. Microbiol. **3**: 112. doi:10.3389/fmicb.2012.00112

Powell, R. T., and A. Wilson-Finelli. 2003. Importance of organic Fe complexing ligands in the Mississippi River plume. Estuar. Coast. Shelf Sci. **58**: 757–763. doi:10.1016/S0272-7714(03)00182-3

Rakshit, S., C. J. Matocha, and G. R. Haszler. 2005. Nitrate reduction in the presence of Wüstite. Soil Sci. Soc. Am. **34**: 1286–1292. doi:10.2134/jeq2004.0459

Risgaard-Petersen, N., S. Rysgaard, and N. P. Revsbech. 1995. Combined microdiffusion-hypobromite oxidation methd for determining nitrogen-15 isotope in ammonium. Soil Sci. Soc. Am. **59**: 1077–1080. doi:10.2136/sssaj1995.03615995005900040018x

Risgaard-Petersen, N., A. Revil, P. Meister, and L. P. Nielsen. 2012. Sulfur, iron-, and calcium cycling associated with natural electric currents running through marine sediment. Geochim. Cosmochim. Acta **92**: 1–13. doi:10.1016/j.gca.2012.05.036

Roberts, K. L., V. M. Eate, B. D. Eyre, D. P. Holland, and P. L. M. Cook. 2012. Hypoxic events stimulate nitrogen recycling in a shallow salt-wedge estuary: The Yarra River Estuary, Australia. Limnol. Oceanogr. **57**: 1427–1442. doi:10.4319/lo.2012.57.5.1427

Roberts, K. L., A. J. Kessler, M. R. Grace, and P. L. M. Cook. 2014. Increased rates of dissimilatory nitrate reduction to ammonium (DNRA) under oxic conditions in a periodically hypoxic estuary. Geochim. Cosmochim. Acta **133**: 313–324. doi:10.1016/j.gca.2014.02.042

Sayama, M., N. Risgaard-petersen, L. P. Nielsen, H. Fossing, and P. B. Christensen. 2005. Impact of bacterial NO3- transport on sediment biogeochemistry. Appl. Environ. Microbiol. **71**: 7575–7577. doi:10.1128/AEM.71.11.7575-7577.2005

Schulz, H. N., and B. B. Jørgensen. 2001. Big bacteria. Annu. Rev. Microbiol. **55**: 105–137. doi:10.1146/annurev.micro.55.1.105

Seitzinger, A. S., J. A. Harrison, J. K. Böhlke, A. F. Bouwman, R. Lowrance, C. Tobias, and G. Van Drecht. 2006. Denitrification across landscapes and waterscapes: A synthesis. Ecol. Soc. Am. **16**: 2064–2090. doi:10.1890/1051-0761(2006)016[2064:DALAWA]2.0.CO;2

Sørensen, J., J. M. Tiedje, and R. B. Firestone. 1980. Inhibition by sulfide of nitric and nitrous oxide reduction by denitrifying *Pseudomonas fluorescens*. Appl. Environ. Microbiol. **39**: 105–108.

Sørensen, J., and L. Thorling. 1991. Stimulation by lepidocrocite of Fe(II)-dependent nitrite reduction. Geochim. Cosmochim. Acta **55**: 1289–1294. doi:10.1016/0016-7037(91)90307-Q

Stookey, L. L. 1970. Ferrozine—a new spectrophotometric reagent for iron. Anal. Chem. **42**: 779–781. doi:10.1021/ac60289a016

Straub, K. L., M. Benz, B. Schink, and F. Widdel. 1996. Anaerobic, nitrate-dependent microbial oxidation of ferrous iron. Appl. Environ. Microbiol. **62**: 1458–1460.

Straub, K. L., and B. E. E. Buchholz-Cleven. 1998. Enumeration and detection of anaerobic ferrous-oxidizing, nitrate-reducing bacteria from diverse European sediments. Appl. Environ. Microbiol. **64**: 4846–4856.

Stumm, W., and J. J. Morgan. 1981. Aquatic chemistry. John Wiley and Sons.

Tai, Y.-L., and B. A. Dempsey. 2009. Nitrite reduction with hydrous ferric oxide and Fe(II): Stoichiometry, rate, and mechanism. Water Res. **43**: 546–52. doi:10.1016/j.watres.2008.10.055

Viollier, E., P. Inglett, K. Hunter, A. Roychoudhury, and P. Van Cappellen. 2000. The ferrozine method revisited: Fe(II)/Fe(III) determination in natural waters. Appl. Geochem. **15**: 785–790. doi:10.1016/S0883-2927(99)00097-9

Vorholt, J., D. Hafenbradl, K. Stetter, and R. Thauer. 1997. Pathways of autotrophic CO2 fixation and of dissimilatory nitrate reduction to N2O in *Ferroglobus placidus*. Arch. Microbiol. **167**: 19–23. doi:10.1007/s002030050411

Weber, K. A., F. W. Picardal, and E. E. Roden. 2001. Microbially catalyzed nitrate-dependent oxidation of biogenic solid-phase Fe(II) compounds. Environ. Sci. Technol. **35**: 1644–1650. doi:10.1021/es0016598

Weber, K. A., J. Pollock, K. A. Cole, M. Susan, O. Connor, L. A. Achenbach, and J. D. Coates. 2006a. Anaerobic nitrate-dependent iron (II) bio-oxidation by a novel lithoautotrophic betaproteobacterium, strain 2002. Appl. Environ. Microbiol. **72**: 686–694. doi:10.1128/AEM.72.1.686

Weber, K. A., M. Urrutia, P. Churchill, R. Kukkadapu, and E. Roden. 2006b. Anaerobic redox cycling of iron by freshwater sediment microorganisms. Environ. Microbiol. **8**: 100–113. doi:10.1111/j.1462-2920.2005.00873.x

Yin, S., D. Chen, L. Chen, and R. Edis. 2002. Dissimilatory nitrate reduction to ammonium and responsible microorganisms in two Chinese and Australian paddy soils. Soil Biol. Biochem. **34**: 1131–1137. doi:10.1016/S0038-0717(02)00049-4

Yin, G., and others. 2014. Denitrification and anaerobic ammonium oxidization across the sediment–water interface in the hypereutrophic ecosystem, Jinpu Bay, in the Northeastern Coast of China. Estuaries Coasts **38**: 211–219. doi:10.1007/s12237-014-9798-1